

# Balanced APD homodyne receiver for quantum applications

Dinka Milovančev, Nemanja Vokić, Florian Honz, Martin Achleitner, Christoph Pacher, and Bernhard Schrenk  
 Center for Digital Safety & Security / Security & Communication Technologies  
 AIT Austrian Institute of Technology,  
 1040 Vienna, Austria  
 {dinka.milovancev, nemanja.vokic, forian.honz, martin.achleitner, chistoph.pacher, bernhard.schrenk}@ait.ac.at

**Abstract**—Performance of linear avalanche photodiode-based balanced homodyne receiver (APD BHD) is examined and compared to reference BHD based on PIN photodiodes, in terms of common mode rejection ratio (CMRR), quantum-to-classical noise clearance (QCNr) and sensitivity in coherent reception of quadrature phase shift keying (QPSK) modulation format. NIST randomness validation was performed on sampled data for quantum random number generator (QRNG). Achieved CMRR values were 50 dB and 30 dB at 100 MHz and 1 GHz, respectively. QCNr of 20 dB at low input power of -20 dBm was demonstrated. Optical sensitivity of APD BHD coherent receiver compared to its PIN BHD counterpart can be improved by 3 dB at low local oscillator (LO) powers, whereas for high LO powers the sensitivity of APD BHD approaches the values for PIN BHD.

**Keywords**—balanced homodyne detectors, avalanche photodiodes, coherent reception, quantum technology

## I. INTRODUCTION

The rise of quantum technologies has brought many applications in recent years especially in the areas of quantum random number generation (QRNG) and quantum key distribution (QKD) as main pillars of digital security. Both areas rely on high performance optical detectors, either single photon avalanche photodiodes (SPAD) and superconducting nanowires or balanced homodyne detectors (BHD) based on PIN photodiodes. The advantage of BHD is its ease of integration into existing communication infrastructure, lower complexity, and higher speed. In this work we are exploring the possibilities of BHD based on avalanche photodiodes (APDs) operated in a linear region where their multiplication gain  $M$  can be adjusted via APD bias. The APD BHD was so

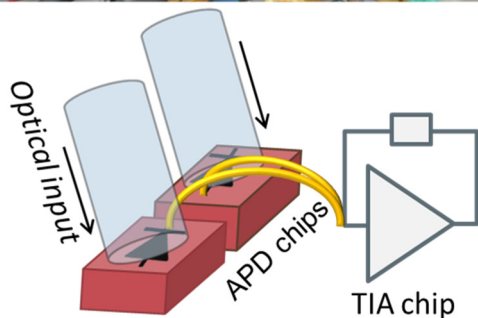
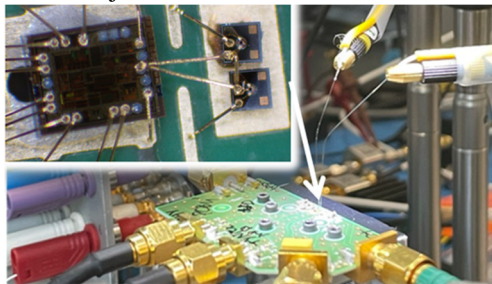


Fig. 1. Balanced APD BHD.

far mainly left unexploited, there has been interest in integrated waveguide coupled balanced APDs but for high-speed data center applications [1]. In the lower frequency regions, recent work on optical time domain reflectometric system [2] used commercial 1550 nm APD BHD with 400 MHz bandwidth (BW) rated for optical coherence tomography.

In this work we aim to increase the bandwidth to allow higher data rates while maintaining low noise levels. By using a die-level subassembly of APDs and low-noise transimpedance amplifier (TIA) (Fig. 1) we could achieve 850 MHz bandwidth at 1550 nm. The characterization of the receiver for quantum applications included the common mode rejection ratio (CMRR), quantum to classical noise clearance evaluation and NIST test on generated random numbers as a quality check. The APD receiver achieved high CMRR (50 dB @ 100 MHz, 30 dB @ 1 GHz), more than 20 dB of clearance even at low input local oscillator (LO) power levels and passing NIST randomness tests [3]. As an initial test of suitability for continuous-variable (CV) QKD, detection of QPSK data with APD BHD as coherent heterodyne receiver was performed. The sensitivity of APD BHD at 500 Mb/s QPSK showed 3 dB improvement over reference PIN BHD but only at very low LO levels (-20 dBm), however at higher LO levels the performance was degraded indicating that very low-noise APDs are needed thus pointing toward 850 nm domain.

## II. APD BHD CHARACTERIZATION – CMRR, CLEARANCE, QRNG OPERATION

### A. APD BHD description

For APD BHD die level assembly design, 10 Gb/s InGaAs APD chips optimized for 1550 nm wavelength were used, the vertical coupling to optical fiber is facilitated through 40  $\mu\text{m}$  active area. The photodiode junction area together with the ground-signal-ground (GSG) pads results in 200 fF capacitance per each APD of the two balanced APDs wire bonded to a commercial low-noise TIA chip rated for 1.25 Gbit/s. The APD noise characteristics such as impact-ionization factor  $k_{\text{eff}}$  and excess noise factor  $F$  are unknown. The excess noise factor is a function of  $k_{\text{eff}}$  and  $M$ , by  $F = M \cdot k_{\text{eff}} + (1 - k_{\text{eff}}) \cdot (1 - 1/M)$ , therefore it increases with  $M$ , which is known as the internal APD gain. The parameter  $M$  and its associated enhanced shot noise are the main separating features from the PIN photodiodes. The APD receiver signal-to-noise ratio (SNR) in case of coherent detection is given by:

$$\begin{aligned}
 \text{SNR} &= \frac{2M^2 R^2 P_S P_{LO}}{\sigma_{th}^2 + \sigma_{Idark}^2 + \sigma_{shot,LO}^2} \\
 &= \frac{2M^2 R^2 P_S P_{LO}}{i_{thermal}^2 \Delta f + 2qFM^2 I_{dark} \Delta f + 2qFM^2 R P_{LO} \Delta f}, \quad (1)
 \end{aligned}$$

where  $q$  – electron charge,  $\Delta f$  – bandwidth,  $i_{thermal}$  – equivalent thermal noise current density of electrical circuitry,  $R$  – low field responsivity,  $P_{LO}$  – local oscillator power,  $P_S$  – signal power and  $I_{dark}$  – unamplified bulk leakage dark current. For good SNR performance, the optimum APD gain  $M$  needs to be found at each  $P_{LO}$ . Regarding the quantum to classical noise clearance, maximum  $M$  will be limited with  $\sigma_{Idark}$  which rises with  $M^2$  and contributes to the classical noise together with thermal noise  $\sigma_{th}$  originating from the TIA; these noise sources are measured when there is no optical input (dark LO), whereas quantum noise is  $\sigma_{shot,LO}$  (lit LO). In case of a PIN receiver,  $M$  and  $F$  are both equal to 1.

### B. Common mode rejection ratio – CMRR

CMRR is measured by modulating the source laser over wide frequency range. The modulated laser power was coupled into one input of fiber-based 3 dB coupler whose outputs were guided to two APDs via two vertically coupled fibers. In the balanced case both fibers contacted the APDs, whereas in unbalanced case only one APD was contacted. The input power was -26 dBm in order not to saturate the TIA in the unbalanced case. The CMRR of 50 dB at 100 MHz and 30 dB up to 1 GHz (Fig. 2a) was possible without using any attenuator to precisely balance the powers; the good balancing was possible by slight adjustment of each APD gain  $M$ , which were set close to 10. The APD BHD 3 dB bandwidth is  $\approx 850$  MHz. For reference, a PIN photodiode-based BHD with the same TIA and fast PIN photodiodes with more symmetrical P/N pads and  $C_{PIN} = 160\text{-}220$  fF achieved CMRR of 35 dB at 100 MHz and 20 dB at 1 GHz (Fig. 2b) using the same setup. Further improvements could be possible by using a planar lightwave circuit (PLC) instead of the fiber-based splitter; the PLC splitter would eliminate potential time skew and splitting mismatch could be compensated with adjustable APD gains. In case of a PIN based BHD, high CMRR over wide frequency range can be dynamically adjusted if photodiodes are implemented on a photonic integrated circuit with Mach-Zehnder modulators as tuning elements [4].

### C. Clearance

Clearance is defined as the ratio of total observable noise to classical noise, whereas the quantum noise corresponds to the difference between total and classical noise. Clearance was

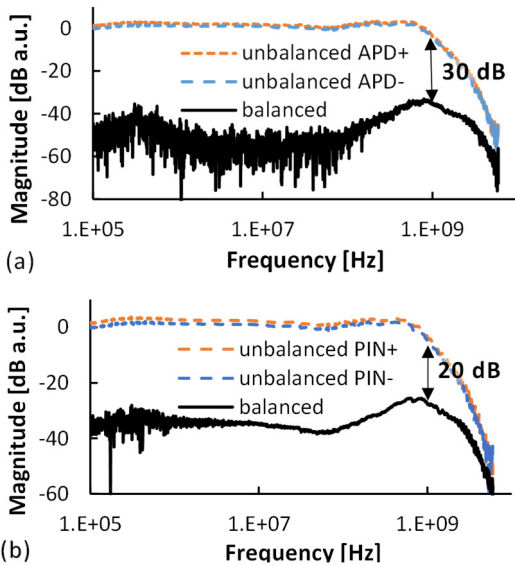


Fig. 2 CMRR measurements of: (a) APD BHD and (b) PIN BHD.

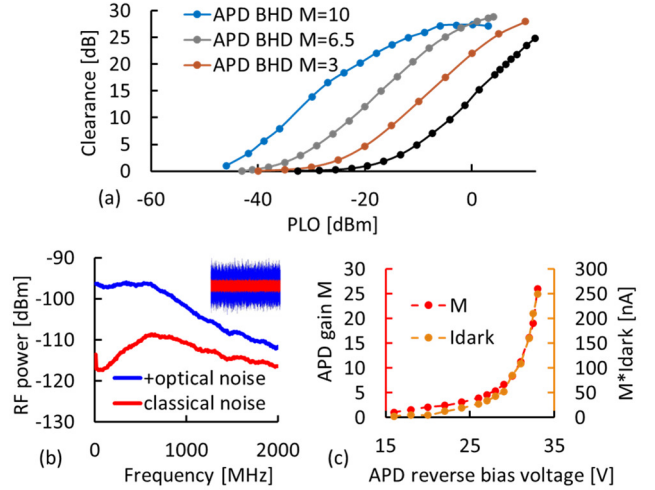


Fig. 3 (a) Clearance at different LO powers (integrated up to 1 GHz); (b) total noise vs. classical noise spectrum and time traces; (c) Multiplication gain and dark current vs. APD reverse bias voltage.

measured using an unmodulated laser source that was fed into 3 dB coupler, while other input port was left unconnected, both output optical ports were coupled to the APD BHD (balanced configuration). For fixed  $M$ , the laser power was swept while TIA output was captured at the oscilloscope. Classical noise is taken as a reference when there is no optical input (dark LO) at each APD bias, while the total noise was measured with lit LO. Clearance curves for different values of  $M$  are shown in Fig. 3a; at each LO power the noise spectrum was integrated up to 1 GHz, the clearance regions that have linear rise with LO power indicate that the noise originates from vacuum fluctuations of light. The spectrum of the classical noise (no optical input) and total noise when optical input is present ( $P_{in} = -10$  dBm,  $M \approx 3$ ) is shown in Fig. 3b. APD BHD can achieve higher clearances at lower LO powers compared to PIN BHD due to its intrinsic  $M$  – the higher the  $M$ , the higher is the clearance increase compared to PIN BHD if operated below saturation power levels. The APD gain cannot be arbitrarily high since the dark current would rise, which increases the classical noise and thus limits the clearance. Additionally, the generated high photocurrents at each APD can lead to saturation. Figure 3c shows the dark current and  $M$  dependence on APD bias. Clearance of up to 20 dB was possible even at low LO powers of -20 dBm when using APD BHD. LO coupling efficiency to the APDs was 60%. High clearance values at low LO powers could prove beneficial in use cases where LO power is split to multiple BHD receivers for multiplexed QRNG operation like it was demonstrated with PIN BHD in [5]. The higher clearance values are desired since these indicate that most of the total noise is indeed quantum shot noise in nature leading to high entropy thus allowing for higher number of extracted random bits from sampled BHD output.

### D. NIST test

In order to evaluate the quality of randomness of the sampled data taken with unmodulated LO as seed, randomness test suite NIST SP800-22-rev1a was used. First, a seeded randomness extraction algorithm used Toeplitz hashing, with the ratio of 0.2 of output to input bit stream lengths; then, 55 samples each with the length of 106 bits were used as an input to NIST test suite consisting of various tests. The exemplary data was acquired at low seed laser power of only -10 dBm and multiplication gain  $M = 3$ , where clearance

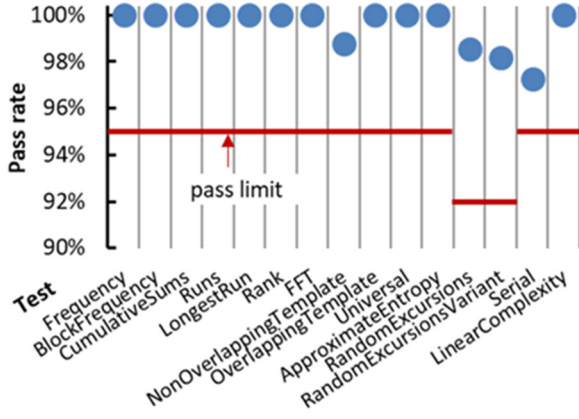


Fig. 4. NIST randomness test suit results.

is above 10 dB (see Fig. 3b). Figure 4 shows that the generated random numbers pass all the NIST tests. For precise estimation of QRNG rate an exact evaluation of min-entropy would be needed, however these clearance results and high available BW of receiver seem promising for Gb/s QRNG rates.

### III. BALANCED APD AS COHERENT RECEIVER

The sensitivity of APD BHD was measured in coherent optical communication scenario which is the basis for CV QKD detection. A simplified heterodyne scheme was used comprising of  $180^\circ$  hybrid (fiber optic 3 dB splitter) and I/Q demodulation in the digital signal processing (DSP), see Fig. 5a. The performance was evaluated at three different LO powers (10  $\mu$ W, 100  $\mu$ W, 500  $\mu$ W). 250 Mbaud QPSK signal data was heterodyned at an intermediate frequency (IF) of 500 MHz (see Fig. 5b). The performance was evaluated for different values of  $M$  (3, 6.5, 10); the BW of APD BHD is constant at these  $M$  values, see Fig. 5c and Fig. 5d. A complementary PIN BHD was again used as a reference. The sensitivity curves show that APD BHD can have a sensitivity improvement of  $\approx 3$  dB compared to PIN BHD only at low LO

powers and low  $M$  (Figs. 5d, 5e, 5f), whereas at higher LO powers there is either no improvement compared to PIN BHD, or the performance is degraded. The PIN BHD sensitivity improved more than 6 dB with increasing LO power, while APD BHD sensitivity improvement is weak (1-2 dB). Nevertheless, due to the low-noise TIA and minimized parasitics, operation close to the FEC limit ( $1 \cdot 10^{-3}$ ) is possible at very low signal levels (below -50 dBm) in most operating settings. The sensitivity curves also show that low APD gains are favored thus pointing to the excess noise factor  $F$  as the limiting parameter for unlocking high sensitivities at high LO powers and high  $M$ . Therefore, unlike for PIN BHD, for APD BHD high clearance values (Fig. 3a) can be misleading in case of sensitivity performance due to its shot noise enhanced nature. To be applicable at highly sensitive application such as CV QKD, APD BHD would need to be operated at high LO powers but with  $M$  close to unity, therefore acting similarly as PIN BHD but with a significant advantage of adjustable  $M$  for achieving high CMRR. For sensitivity performance gains we need an improved noise performance of the used APDs, typically for InGaAs  $F \approx 5$  at typical gain of  $M = 10$ , whereas silicon based APDs reach similar value of  $F$  at an order of magnitude higher  $M$  values ( $M \sim 100-150$ ), the difference is also evident by looking into  $k_{eff}$ , whose typical value is 0.02 for Si and 0.45 for InGaAs APDs. Therefore, 850 nm region where low-noise silicon APDs are available should be investigated. For 1550 nm region, another APD option could be InAs APD with  $F$  below 2 irrespective of the applied  $M$  [6], but these APDs have been so far only reported in literature and are not commercially available.

### IV. CONCLUSION

We evaluated performance of die-level APD BHD in terms of important metrics for certain quantum applications and compared it to a reference PIN BHD. The obtained high clearance values at low LO powers could find applicability in QRNG applications. The sensitivity measurements, however, indicate that APD BHD does not offer advantage over PIN and that its gain  $M$  would be detrimental at high LO since the

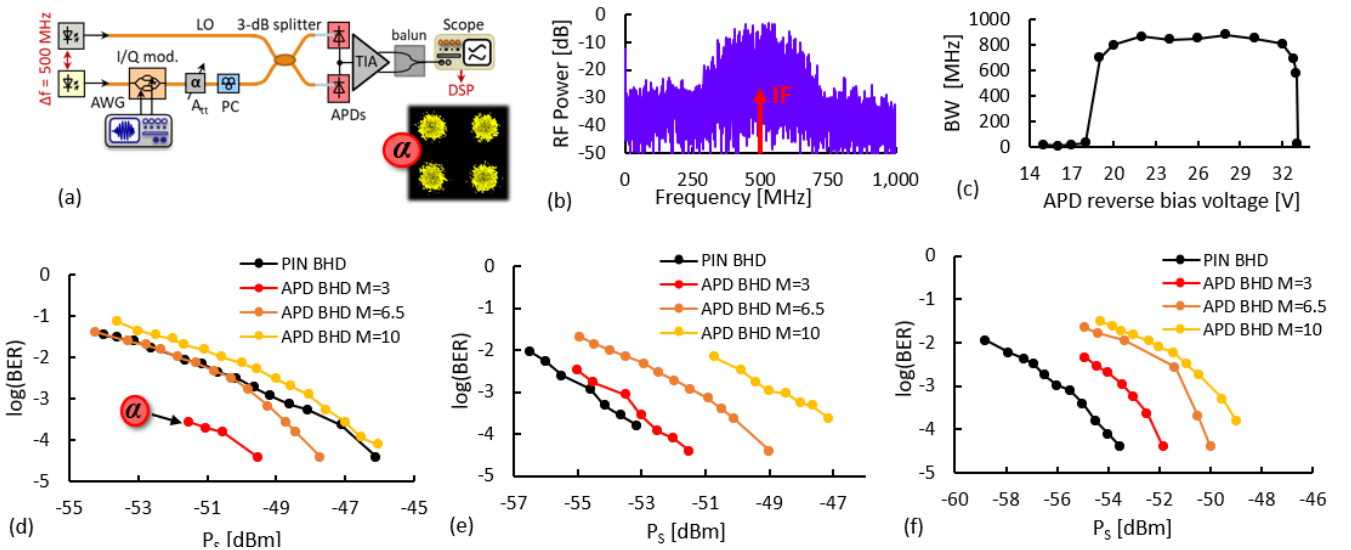


Fig. 5. (a) Measurement setup, (b) heterodyned QPSK spectrum, (c) BW vs. APD reverse bias voltage, sensitivity curves for 250 Mbaud QPSK at (d)  $P_{LO} = 10 \mu$ W, (e)  $P_{LO} = 100 \mu$ W, (f)  $P_{LO} = 500 \mu$ W.

excess noise  $F$  of standard InGaAs APDs is too high. At high LO powers only the operation at  $M$  close to unity with the added value of high CMRR could be an option for APD BHD. For future work the estimation of min-entropy for QRNG application needs to be performed as well as investigation of low-noise balanced silicon APDs optimized for 850 nm.

#### ACKNOWLEDGMENT

This work was supported in part by the ERC under the EU Horizon-2020 programme (grant agreement No 804769) and by the Austrian Research Promotion Agency FFG (n° 884443).

#### REFERENCES

- [1] T. Beckerwerth, F. Ganzer, P. Runge and M. Schell, "High-Speed Balanced Avalanche Photodetector for Homodyne Detection," *2019 Conference on Lasers and Electro-Optics Europe & European Quantum Electronics Conference (CLEO/Europe-EQEC)*, Munich, Germany, 23-27 June 2019.
- [2] T.-T. Lin, Y.-X. Bai, Z.-C. Zhong, and X. Gao, "Phase-Sensitive Optical Time-Domain Reflectometric System Based on Optical Synchronous Heterodyne," *IEEE Sensors Journal*, vol. 21, no. 10, pp. 12130-12136, May 2021.
- [3] National Institute of Standards and Technology (NIST), Technology Administration, U.S. Department of Commerce, "A Statistical Test Suite for Random and Pseudorandom Number Generators for Cryptographic Applications," Special Publication 800-22, revision 1a, 2010.
- [4] C. Bruynsteen, M. Vanhooeck, J. Bauwelinck, and X. Yin, "Integrated balanced homodyne photonic-electronic detector for beyond 20 GHz shot-noise-limited measurements," *OSA Optica*, vol 8, no. 9, pp. 1146-1152, Sep. 2021.
- [5] B. Haylock, D. Pease, F. Lenzini, C. Weedbrook, and M. Lobino, "Multiplexed Quantum Random Number Generation," *Quantum Journal*, vol. 3, Art. no. 141, 2019.
- [6] S. J. Maddox, W. Zun, Z. Lu, N. P. Nair, J. C. Campbell, and S. R. Bank, "Enhanced low-noise gain from InAs avalanche photodiodes with reduced dark current and background doping," *AIP Applied Physics Letters*, vol. 101, Art. no. 151124, Oct. 2012.